

Off-Line and On-Line Fatigue Crack Growth Prediction Using Multivariate Gaussian Process

Subhasish Mohanty¹, Aditi Chattopadhyay², Pedro Peralta³,
Arizona State University, Tempe, AZ, 85287, USA

Santanu Das⁴
NASA Ames Research Center, Moffett Field, CA, 94035, USA

Off-line and On-line fatigue crack growth prediction of Aluminum 2024 compact-tension (CT) specimens under variable loading has been modeled, using multivariate Gaussian Process technique. The Gaussian Process model projects the input space to an output space by probabilistically inferring the underlying non-linear function relating input and output. For the off-line prediction the input space of the model is trained with parameters that affect fatigue crack growth, such as number of fatigue cycles, minimum load, maximum load, and load ratio. For the case of online prediction, the model input space is trained using features found from piezoelectric sensor signals rather than training the input space with loading parameters, which are difficult to measure in a real time scenario. Two different algorithms such as Principal Component Analysis (PCA) and Kernel Principal Component Analysis (KPCA) are used to extract the principal features from sensor signals. In both the off-line and on-line case the output space is trained with known associated crack lengths. Once the Gaussian process model is trained, a new output space for which the corresponding crack length or damage state is not known is predicted using the trained Gaussian process model. Concepts are validated through several numerical examples.

Nomenclature

a_i	= i^{th} random crack length
a_{N+1}	= $N+1^{\text{th}}$ test (unknown) crack length
\mathbf{C}_d	= $d \times d$ covariance matrix for PCA feature extraction
D	= $\{\mathbf{x}_i, a_i\}_{i=1}^N$ Gaussian Process training space
d	= Input dimension
M	= Number of sensor observation used for PCA or KPCA at any fatigue cycle instances
N	= Number of different fatigue cycle instances
\mathbf{K}_N	= $N \times N$ kernel matrix for Gaussian Process input-output space mapping
\mathbf{K}_d	= $d \times d$ kernel matrix for Kernel PCA feature extraction
\mathbf{x}_i	= $d \times 1$ i^{th} Fatigue instances input vector
\mathbf{x}_{N+1}	= $d \times 1$ $N+1^{\text{th}}$ test input vector
\mathbf{y}_d	= $1 \times d$ Sensor observation

¹ Graduate Research Associate, Mechanical & Aerospace Engineering, subhasish.mohanty@asu.edu.

² Professor, Mechanical & Aerospace Engineering, aditi@asu.edu, Fellow AIAA.

³ Associate Professor, Mechanical & Aerospace Engineering, pperalta@asu.edu.

⁴ Associate Scientist, Intelligent Data Understanding, sdas@arc.nasa.gov.

Report Documentation Page				Form Approved OMB No. 0704-0188	
Public reporting burden for the collection of information is estimated to average 1 hour per response, including the time for reviewing instructions, searching existing data sources, gathering and maintaining the data needed, and completing and reviewing the collection of information. Send comments regarding this burden estimate or any other aspect of this collection of information, including suggestions for reducing this burden, to Washington Headquarters Services, Directorate for Information Operations and Reports, 1215 Jefferson Davis Highway, Suite 1204, Arlington VA 22202-4302. Respondents should be aware that notwithstanding any other provision of law, no person shall be subject to a penalty for failing to comply with a collection of information if it does not display a currently valid OMB control number.					
1. REPORT DATE 2008		2. REPORT TYPE		3. DATES COVERED 00-00-2008 to 00-00-2008	
4. TITLE AND SUBTITLE Off-Line and On-Line Fatigue Crack Growth Prediction Using Multivariate Gaussian Process				5a. CONTRACT NUMBER	
				5b. GRANT NUMBER	
				5c. PROGRAM ELEMENT NUMBER	
6. AUTHOR(S)				5d. PROJECT NUMBER	
				5e. TASK NUMBER	
				5f. WORK UNIT NUMBER	
7. PERFORMING ORGANIZATION NAME(S) AND ADDRESS(ES) Arizona State University ,Department of Mechanical & Aerospace Engineering,Tempe,AZ,85287				8. PERFORMING ORGANIZATION REPORT NUMBER	
9. SPONSORING/MONITORING AGENCY NAME(S) AND ADDRESS(ES)				10. SPONSOR/MONITOR'S ACRONYM(S)	
				11. SPONSOR/MONITOR'S REPORT NUMBER(S)	
12. DISTRIBUTION/AVAILABILITY STATEMENT Approved for public release; distribution unlimited					
13. SUPPLEMENTARY NOTES AIAA Journal, 2008, submitted					
14. ABSTRACT					
15. SUBJECT TERMS					
16. SECURITY CLASSIFICATION OF:			17. LIMITATION OF ABSTRACT Same as Report (SAR)	18. NUMBER OF PAGES 23	19a. NAME OF RESPONSIBLE PERSON
a. REPORT unclassified	b. ABSTRACT unclassified	c. THIS PAGE unclassified			

I. Introduction

Aircraft maintenance must balance labor, logistic, and equipment budget constraints with the competing requirements of fleet readiness, reliability, and safety. Recently, stringent Diagnostic, Prognostic, and Health Management (PHM) capability requirements are being placed on new applications, like the Joint Strike Fighter (JSF)[1], in order to enable and reap the benefits of new and revolutionary Logistic Support concepts. Though the Prognostics and Health Management (PHM) [2] is the name given to the capability being developed by JSF to enable the vision of Autonomic Logistics and so meet the overall affordability and supportability goals, similar PHM systems can be developed and implemented for residual life prognostics and health management of any civil, mechanical or aerospace structure. Currently aggressive research is going on for development of an integrated PHM system, however these research activities are generally in an incipient stage to address the stringent requirement of a truly effective PHM system. Current aerospace practice follows a damage-tolerant reliability engineering model whereby structural components are regularly inspected and replaced. The replaced components are not necessarily at the end of its designed strength. These practices unnecessarily add to the overhauling expenditure and time. The damage-tolerant reliability engineering designs are generally based on a physics-based fracture mechanics approach or a data driven stochastic approach. The physics-based damage tolerance approach that is widely practiced [3-6] and constantly been improved is primarily based on linear fracture mechanics (LFEM), as far as fatigue failure is concerned. Another form of damage tolerance approach, known as a life usage model [7,8], is also widely used and is based on gathering statistical information about how long a component endures before failure, and uses these statistics, collected from a large population sample, to make remaining life predictions for individual components. However, these predictions are not based on measured characteristics of the individual components. In addition, fatigue life of aircraft structural components under service loading condition [9,10] is often analyzed and predicted based on crack growth rates obtained from constant-amplitude fatigue testing data. In contrast to the fatigue crack growth due to constant amplitude loading, crack growth caused by variable amplitude loadings is characterized by retardation and acceleration effects [11], which extend or reduce the lifetime of structures. Currently there are many physics-based models [3-6, 12, 13] with empirical parameters available to model crack growth with retardation and acceleration effects. These models reasonably capture the dynamics of the fatigue crack growth under variable loading in a deterministic framework. However, these models do not explicitly model the uncertainty in crack

growth that arises due to scatter [9,10] in micro-structural properties and subsequent uncertainty propagation due to loading sequence effects.

As of today many research works varying from medical application [14] to aerospace application [15] show the effective use of neural network for diagnostic and prognostic systems. However few of these neural network models are based on the explicit uncertainty quantification approach like the Bayesian uncertainty modeling approach. It is noted that Bayesian methods allow [16] complex neural network models to be used without fear of the “over fitting” that can occur with traditional neural network learning methods. However the Bayesian analysis of neural networks is difficult [17] because a simple prior over weighing parameters of the network requires a complex prior over underlying functions and, hence, it becomes computationally intractable. The present paper discusses the use of the Gaussian Process approach [17, 18] for a prognostic system that explicitly models Bayesian uncertainty into the predictive model. A Gaussian process (GP) model is a simplification of Bayesian analysis of neural networks by assuming that the multivariate random variables are gaussian random variables in an infinite (countable or continuous) index set. The Gaussian process model projects the input space to an output space by probabilistically inferring the underlying non-linear function relating input and output.

In the present paper both offline and online predictions of fatigue crack growth in Compact Tension (CT) samples are made using a multi variate Gaussian process model. For off-line prediction the input space of the model is trained with parameters that affect fatigue crack growth such as, number of fatigue cycles, minimum load, maximum load, and load ratio. In turn, the output space is linked to the corresponding crack lengths or crack growth rates. The Gaussian Process, models the scatter in fatigue crack growth that arises due to microstructural variability, loading uncertainty and variability due to manufacturing tolerance. Once the Gaussian process is trained with a known input-output data set, it can predict the output crack length or its rate under the particular loading envelope. For the case of online prediction, the model input space is trained using features found from piezoelectric sensor signals rather than training the input space with loading parameters, whereas, the output space is trained with corresponding crack lengths. The sensor features are found using either Principal Component Analysis (PCA) [19, 20] or Kernel Principal Component Analysis (KPCA) [21].

II. Technical Approach

The following section outlines a general approach for a hybrid prognosis model with a detail description on off-line data driven predictive model and system identification based on-line predictive model.

A. General Overview on Hybrid Prognosis Model

A hybrid prognosis model based on both physics and data driven based techniques is being developed. A schematic of the hybrid prognosis model is shown in Fig. 1. The overall prognosis model will have three different modules: off-line physics based model, off-line data driven probabilistic model and system identification based an on-line predictive model. All the three sub modules will be finally integrated together to develop a hybrid prognosis model. The off-line physics-based predictive model will be based on a non-linear fracture mechanics based approach, whereas the off-line data driven model and on-line system identification model will be based on a probabilistic Gaussian process approach. The off-line data driven model will explicitly model the macro level uncertainty that arises due to microstructure variability, loading uncertainty, etc., and complement the off-line physics based model for any unmodeled exogenous influences. The physics-based model combined with data driven probabilistic model will be used for off-line prediction of residual useful life of a structural components under an anticipated flight envelope, whereas piezoelectric sensor signal based online predictive model will estimate the current damage state in real time and make this information available to off-line module to reassess the residual useful life of the component based on those real time information. The present paper discusses only on the predictive capability of data driven based off-line and on-line predictive model.

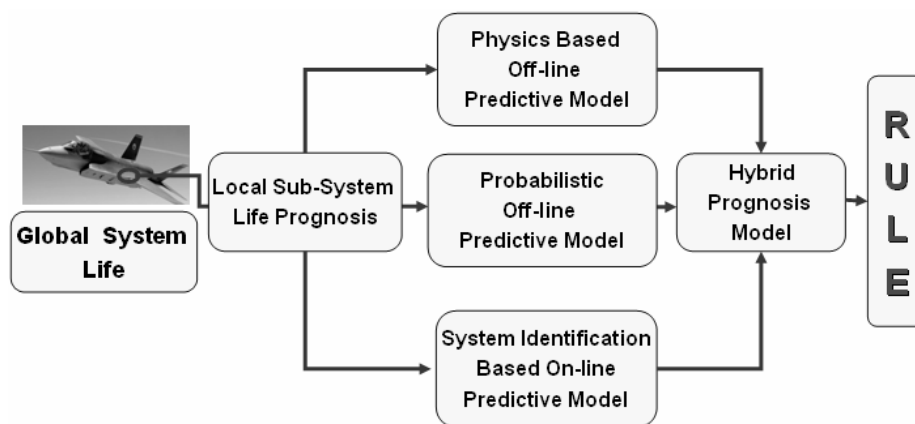


Fig. 1 A conceptual hybrid prognostic model (Source of the fighter plane image in figure is from <http://www.jsf.mil>).

B. Gaussian Process Based Off-line Predictive Model

The goal of Gaussian process data driven prediction model is to compute the distribution of damage state for future instances for which the damage affecting physical parameters are known. For example, the loading patterns, number of flight cycles elapsed, initial damage size, environmental condition, grain size distributions are the typical damage affecting physical parameters. The Gaussian process assumes the scatter in crack growth (as schematically shown in Fig. 2) is due to variation in these parameters. Due to the scatter in crack length or the damage state, at any instances the damage state follows a distribution rather than being deterministic. Gaussian process assumes this individual distribution as Gaussian distribution with different mean and variance and evaluates the conditional distribution of future damage state ($N+1^{\text{th}}$ test damage state as depicted in Fig. 2) as $f(a_{N+1} | D = \{\mathbf{x}_i, a_i\}_{i=1}^N, \mathbf{x}_{N+1})$, i.e., to compute the probability distribution of the damage state a_{N+1} given a test input \mathbf{x}_{N+1} and a set of ' N ' training

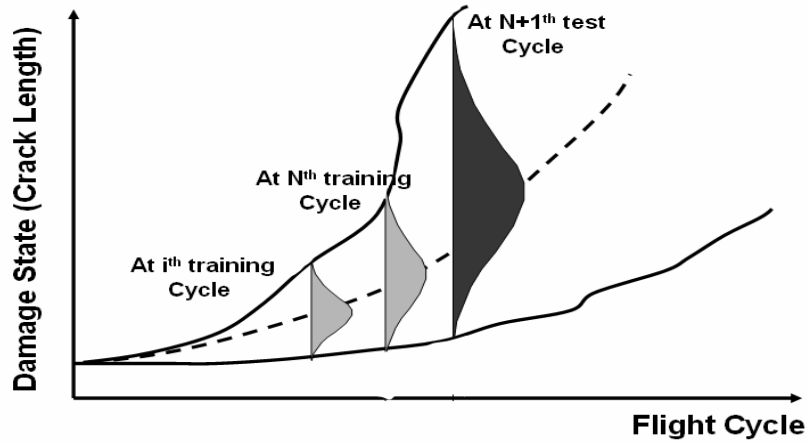


Fig 2 Individual distributions at various instances of time those collectively make Gaussian Process.

points $D = \{\mathbf{x}_i, a_i\}_{i=1}^N$. The a_i is the i^{th} random variable at i^{th} fatigue cycle. Let us define our damage state data vector $\{a_i\}_{i=1:N}$ to be a Gaussian process with a kernel matrix \mathbf{K}_N . By doing this we have bypassed [17, 18] the step of expressing individual priors on the noise and the modeling function by combining both priors into the kernel matrix \mathbf{K}_N . Now the Gaussian distribution over a_{N+1} [17, 18, 22] can be written as

$$f(a_{N+1} | D, \mathbf{K}_N(\mathbf{x}_i, \mathbf{x}_j), \mathbf{x}_{N+1}, \Theta) = \frac{1}{Z} \exp \left(-\frac{(a_{N+1} - \hat{a}_{N+1})^2}{2\sigma_{\hat{a}_{N+1}}^2} \right) \quad (1)$$

Where Z is an appropriate normalizing constant and the mean and variance of the new distribution are, respectively, defined as:

$$\hat{a}_{N+1} = \mathbf{k}_{N+1}^T \mathbf{K}_N^{-1} \mathbf{a}_N ; \sigma_{\hat{a}_{N+1}}^2 = \kappa - \mathbf{k}_{N+1}^T \mathbf{K}_N^{-1} \mathbf{k}_{N+1} \quad (2)$$

In Eq. (2) \mathbf{a}_N is the $(1 \times N)$ training output vector that is here the crack length. Whereas, κ , \mathbf{k}_{N+1} , \mathbf{K}_N are the partitioned components of $N+1^{\text{th}}$ instances kernel matrix \mathbf{K}_{N+1} and can respectively described as

$$\kappa = k(\mathbf{x}_{N+1}, \mathbf{x}_{N+1}) ; k_i = k(\mathbf{x}_{N+1}, \mathbf{x}_i)_{i=1,2,\dots,N} ; K_{i,j} = k(\mathbf{x}_i, \mathbf{x}_j)_{i,j=1,2,\dots,N} \quad (3)$$

In Eq. (3) k is the assumed kernel function. There are many possible choices of prior kernel functions. From a modeling point of view, the objective is to specify a prior kernel that contains our assumptions about the structure of the process being modeled. Formally, we are required to specify a function that will generate a positive definite kernel matrix for any set of inputs. A non-stationary multi-layer perceptron [23] kernel function is used for the current Gaussian Process model and is given by:

$$k(\mathbf{x}_i, \mathbf{x}_j) = \Theta_1 \sin^{-1} \left(\frac{(\mathbf{x}_i)^T \Theta_2 (\mathbf{x}_j)}{\sqrt{(1 + (\mathbf{x}_i)^T \Theta_2 (\mathbf{x}_i))} \sqrt{(1 + (\mathbf{x}_j)^T \Theta_2 (\mathbf{x}_j))}} \right) + \Theta_3 \quad (4)$$

The parameters $\Theta_{i=1,2,3}$ are adjusted to maximize the log likelihood L , given by

$$L = -\frac{1}{2} \log \det \mathbf{K}_N - \frac{1}{2} \mathbf{a}_N^T \mathbf{K}_N^{-1} \mathbf{a}_N - \frac{N}{2} \log 2\pi \quad (5)$$

These hyperparameters are initialized to reasonable values and then, the conjugate gradient method is used to search for their optimal values. Initially the kernel function given in Eq. (4) is evaluated using the assumed initial hyperparameters and the input space vectors \mathbf{x}_i . The input space vectors \mathbf{x}_i is a 'd' dimensional vector with individual elements of the vector contains the value of the different fatigue affecting parameters at the i^{th} instances. Whereas, 'd' is the number of fatigue affecting physical parameters for off-line predictive model and dimension of sensor signal feature vector for on-line predictive model.

C. Gaussian Process Based On-line Predictive Model

In the last section we discussed the off-line prediction with a Gaussian process input space generated from loading change information and other fatigue parameters. However, in real time it is hardly possible to measure loading or compliance change information in a component that is already assembled into full scale flight hardware. This is because the load cells are usually large and heavy and in a multi-axial loading environment it is impossible to measure the loading change information. However, we can mount small piezoelectric sensors in the full scale hardware to measure equivalent loading and associated compliance change information in a real time situation. These sensor signals can be obtained at regular instances and after required processing can be fed to the Gaussian Process input space to map input space to output space crack length or crack growth rate. Once the training input space and training output space formed using Eq. (1) to Eq. (5) we can find the new predicted mean and variance for a new test input space. A general architecture for on-line prediction model is shown in Fig.3. The figure shows the

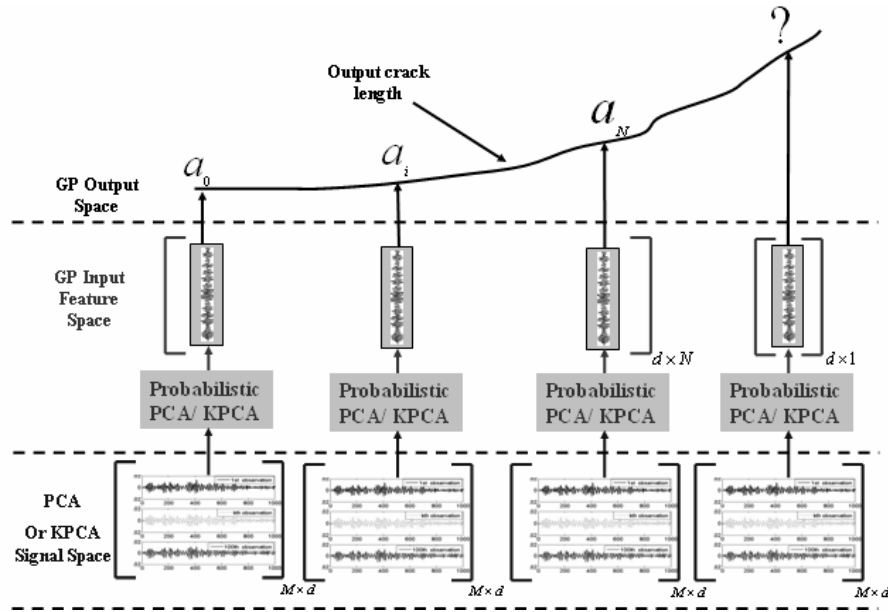


Fig. 3 General architecture for on-line predictive model

multiple sensor signals that are collected at different instances of a fatigue loading envelop. These signals form the signal space for the feature extraction algorithms, such as Principal Component Analysis (PCA) or Kernel Principal Component Analysis (KPCA). The feature extraction algorithm statistically denoises the original signal and

generates ranked feature vectors ordered according to its information content. Once the feature vector is found it can fed to the Gaussian Process input space to map the original sensor signal with the corresponding crack length or crack growth rate. The detail of the feature extraction algorithms are discussed below.

1. Principal Component Analysis (PCA)

Principal component analysis [19, 20] is an orthogonal basis transformation that has been widely used for multivariate data analysis and dimensionality reduction. Intuitively, PCA is a process that identifies the direction of the principal components where the variance of changes in dynamics is maximum. Assuming ‘M’ different observations and each observation with d dimensions (as described in Fig. 3) each input signal space \mathbf{y}_p vector is a $M \times 1$ vector. It is noted that each sensor observation is a $1 \times d$ vector named as \mathbf{y}_d . Then the centered $d \times d$ covariance matrix of the data set $\{\mathbf{y}_p \in R^M \mid p = 1, 2, \dots, d\}$ can be found as

$$\mathbf{C}_d = \langle (\mathbf{y}_q - \langle \mathbf{y}_p \rangle) (\mathbf{y}_q - \langle \mathbf{y}_p \rangle)^T \rangle \quad (6)$$

Then the covariance matrix is diagonalized to obtain the principal components and the diagonalization can be performed by solving the following eigenvalue problem:

$$\lambda \mathbf{v} = \mathbf{C}_d \mathbf{v} \quad (7)$$

The coordinates in the eigenvector basis are called principal components. The size of an eigenvalue λ corresponding to an eigenvector \mathbf{v} of covariance matrix \mathbf{C}_d equals the amount of variance in the direction of \mathbf{v} . Furthermore, the direction of the first ‘n’ eigenvectors corresponding to the largest ‘n’ eigenvalues covers as much variance as possible by ‘n’ orthogonal directions. For the present on-line prediction problem the first eigenvector is considered to be the most pristine quantity with maximum buried information and called the principal feature vector. This $d \times 1$ feature vector corresponds to the i^{th} instances input vector \mathbf{x}_i of the Gaussian process input space.

2. Kernel Principal Component Analysis (KPCA)

One cannot assert that the linear PCA will always detect all structures in a given data set. By the use of suitable nonlinear features, one can extract more information. Kernel PCA (KPCA) [21] is well suited to extract non-linear structures in the data. Kernel PCA extends the above mentioned PCA approach, and performs principal component

analysis in a high dimensional space. For the purpose the original data given by $\{\mathbf{y}_p \in R^M \mid p = 1, 2, \dots, d\}$ are first mapped into a high dimensional space F via a (usually nonlinear) mapping Φ and then a linear PCA is performed on the mapped data. Then the $d \times d$ covariance matrix of the new mapped data set can be found as

$$\mathbf{K}_{i,j} = (\Phi(\mathbf{x}_i), \Phi(\mathbf{x}_j)) = k(\mathbf{x}_i, \mathbf{x}_j) \quad (8)$$

There are many form of kernel function. For the present feature extraction problem a radial basis function (RBF) [18, 21] based kernel function is used, which has the following form:

$$k(\mathbf{x}_i, \mathbf{x}_j) = \exp\left(-\frac{\|\mathbf{x}_i - \mathbf{x}_j\|^2}{\Theta}\right) \quad (9)$$

Where, the hyperparameter Θ is assumed constant. Then the kernel matrix is diagonalized to obtain the principal components and the diagonalization can be performed by solving the following eigenvalue problem:

$$\lambda \mathbf{v} = \mathbf{K} \mathbf{v} \quad (10)$$

Where λ and \mathbf{v} are respectively the eigenvalue and eigenvector. Also in a similar way as described for PCA based feature extraction technique, the first feature vector from every Kernel PCA analysis can be used to feed the Gaussian process input space.

III. Numerical Verification

Numerical studies have been conducted to verify the effectiveness of the developed prediction model by using experimental data obtained from fatigue tests conducted in-house. The details of the experiment and numerical studies are discussed below.

A. Fatigue Test Experiment

The fatigue experiments were performed using an Instron 1331 servo-hydraulic load frame operating at 20 Hz. Eighteen Al 2024 T351 Compact Tension (CT) samples, each 6.31 mm thick, were used. These specimens were fabricated according to ASTM E647-93 with an average width of 25.53 mm (from the center of the pin hole to the edge of the specimen) and an average height of 30.6 mm. To simulate typical flight loading conditions a variable load spectrum was programmed into the digital controller of the load frame. The spectrum, as coded to the load-cell,

is shown in Fig. 4. However, due to noise and compliance effects the load that was actually applied to structure was somewhat different than that programmed to the controller. The minimum and maximum loads applied to the

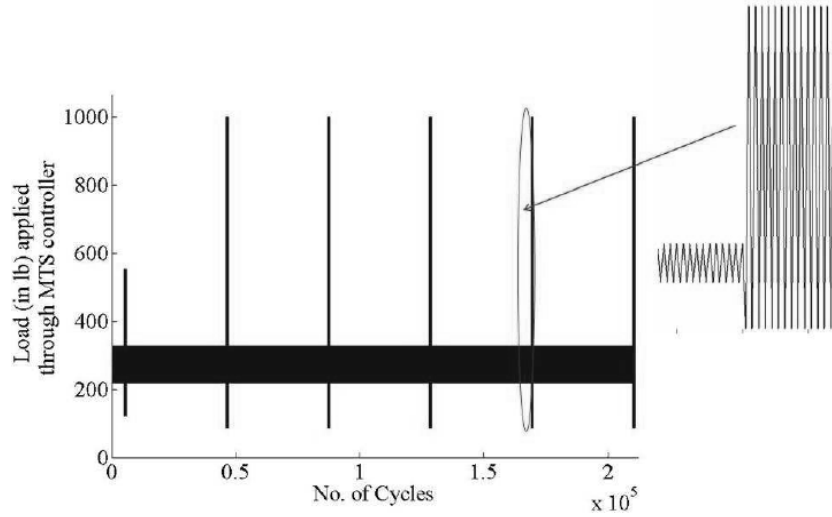


Fig. 4 Loading spectrum programmed to load frame controller

structure were measured through the load cell and are used to construct the Gaussian process input space. It must be noted that for each sample the frame was stopped and the corresponding load cell outputs were recorded at chosen instances during the experiment. Each time the test was stopped, a high resolution picture of the cracked sample was taken using a digital camera to generate the output space crack length data. The corresponding measured crack lengths for different samples are depicted in Fig. 5. It is noted that CT samples are named from ct416a to ct436a.

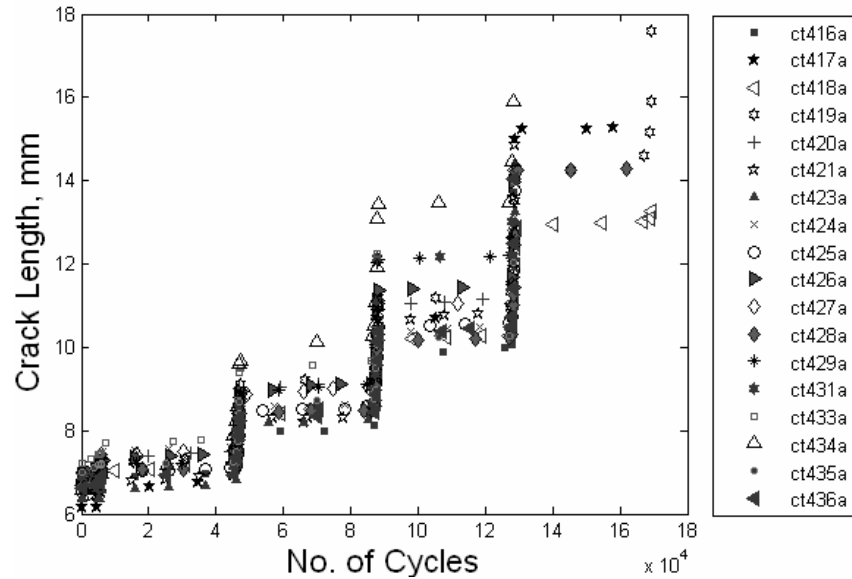


Fig. 5 Experimental crack length data

The prefix ‘ct’ symbolizes compact tension, the middle number shows the number of the sample, and the suffix ‘a’ indicates that the initial notch is made along the rolling direction of the aluminum plate. The absence of some numbers, such as ct422a (Fig. 5) imply that the data could not be collected for those samples due to premature failure of the specimen. Out of a total of 18 samples for which the fatigue crack length data were available, four samples: ct417a, ct419a, ct421a and ct423a were instrumented with a piezoelectric sensor and an actuator. A typical instrumented sample after the fatigue test is shown in Fig. 6. When the test frame was stopped the piezoelectric actuator was excited with a narrow band burst signal. The corresponding sensor signal was collected using a National Instrument (NI) data acquisition system. These collected signals are used as input to the on-line predictive model, which will be discussed in detail later. The CT specimens were not removed from the test frame and were kept under tensile static loading condition during this sensor data collection process to simulate realistic on-board conditions. At each stopping instant, 150 sensor observations were collected, out of which 100 were selected based on a Fast Fourier Transform (FFT) filter. These 100 observations were used as inputs to PCA or KPCA algorithms for feature extraction at those instances.

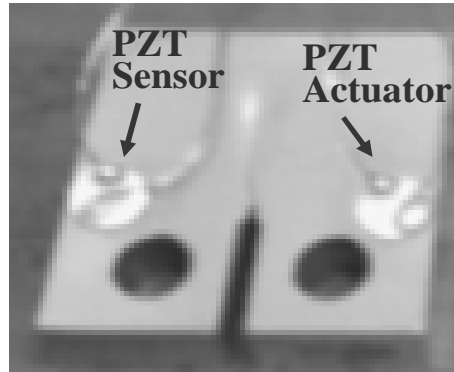


Fig. 6 Instrumented CT specimen

B. Gaussian Process Off-line Prediction

The Gaussian process input spaces are constructed using the load cell readings at different instances and the fatigue cycles at those instances. The individual \mathbf{x}_i is a $d \times 1$ vector with elements comprising fatigue cycles, minimum load, maximum load and load ratio. The individual \mathbf{x}_i form the $d \times N$ input training space and the corresponding $1 \times N$ observed crack lengths (from high resolution images) form the training output space. The dimension of the input space can be varied to any number, but for the present study it is restricted to one for single

variate predictions and four for multivariate predictions. For a new test instance with known input \mathbf{x}_i the corresponding mean output crack length is predicted using Eq. (2). Before using the data for GP prediction the input and output space variables are logarithmically scaled. In addition to following a zero mean Gaussian process as described in Eq. (1), the output crack lengths are scaled as zero mean random data. Both the single and multivariate predictions of output crack lengths are made for all 18 CT specimen (ref. Fig. 5). It is noted that while selecting a

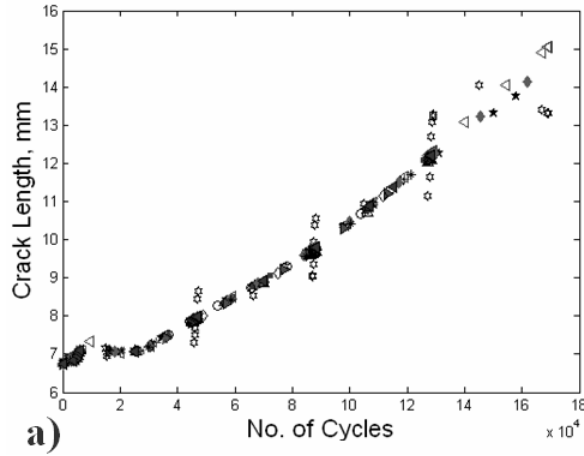


Fig. 7a Single variate prediction

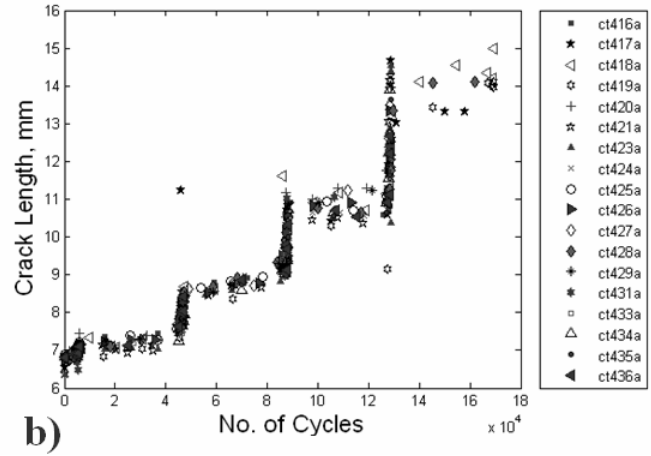


Fig. 7b Multi variate prediction

particular sample as a test specimen, the data from rest of the seventeen samples are used for training the Gaussian process model. Figures 7A and 7B show the single variate and multivariate GP predictions of crack length, respectively. Comparing Fig. 7A and 5, it can be seen that even though the single variate GP with time (number of cycles) as only one input variable is able to predict an average crack growth curve, it is unable to track the transient jump in crack growth that arises due to transient over load cycles (Fig. 4). The only exception is sample ct419a where a good prediction is observed (ref. Fig. 7A). However, comparing Fig. 7B and 5 it can be seen that the multivariate GP captures those transient loading effects for most of the samples. To further improve the GP off-line prediction, a rate-based prediction has been also performed. In this case, rather than predicting directly the crack length, the crack growth rate is predicted first, and then it is integrated using time as the only input variable, and the corresponding crack length is estimated. From a numerical perspective, it is better to predict a derivative than to predict an integral (here, the crack length) for a highly non-smooth function. Also from a physical perspective, fatigue crack growth is normally expressed in terms of a first order nonlinear rate equation. Therefore, although the direct crack length based GP model is capable of capturing the nonlinearity, the rate-based prediction allows capturing first order crack growth rate, and helps capture the physics of a dynamic system. However, it must be

noted that to perform a rate-based crack growth estimation, the cycle by cycle rate has to be integrated for the most correct crack growth curve estimation. In the present case, where experimental data were available only at discrete instances, the prediction of crack growth rate is possible at only those instances for which the input space variables are available from experimental observation. Nevertheless, to estimate a continuous crack length curve in the cycle by cycle integration process when the crack growth rate is not available at a particular cycle, the crack growth rate for a previous cycle is assumed for the current cycle. A comparison of GP prediction of crack growth rate and the crack growth rate observed from experiments can be seen in Figs. 8A and 8B. The figures show that with the exception of a slightly lower rate prediction compared to the experimental rate, there is a good correlation between predicted and observed

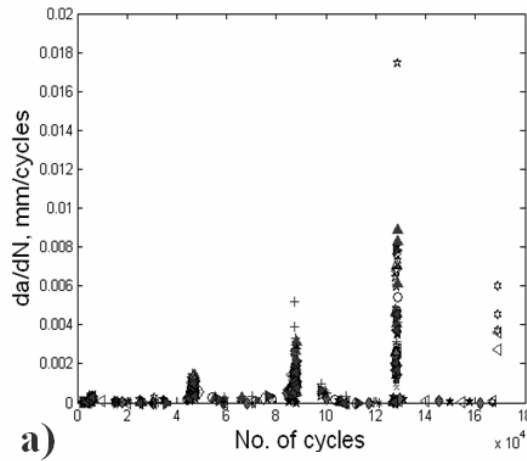


Fig. 8a Predicted rate from multivariate GP

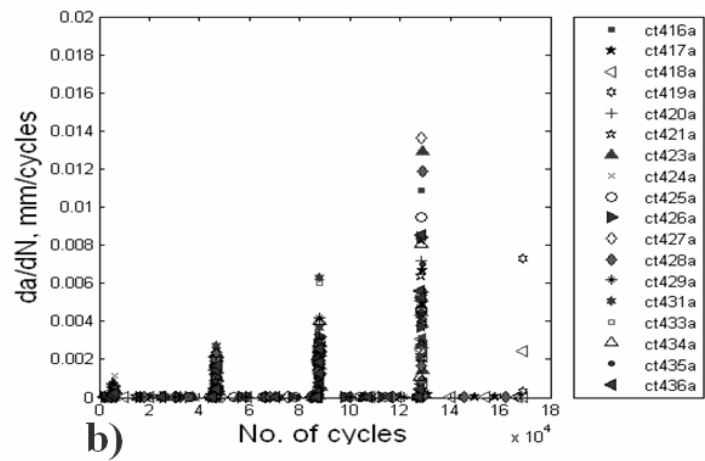


Fig. 8B Rate from experimental observation

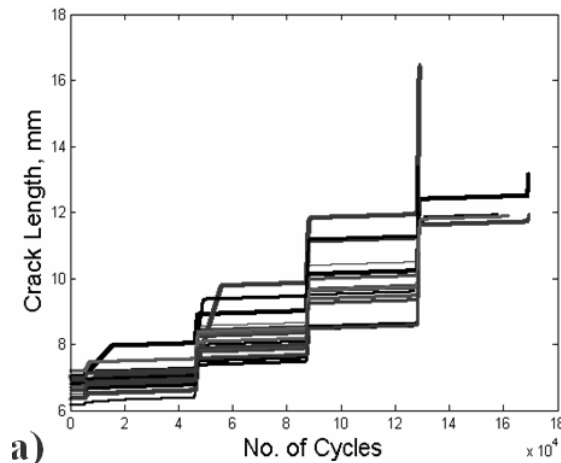


Fig. 9a Continuous crack length from integration of GP estimated rate

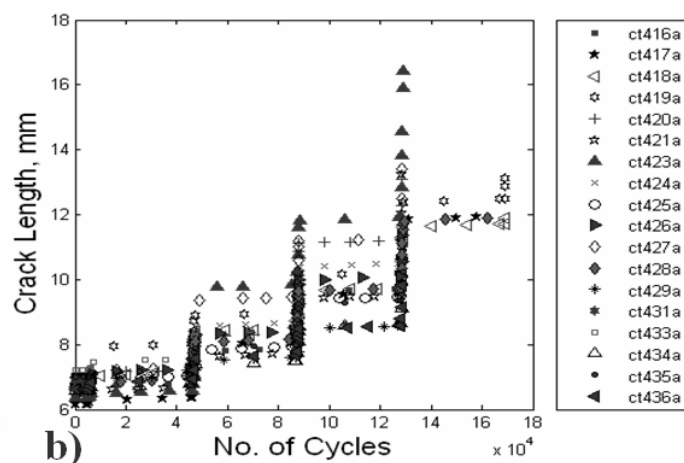


Fig. 9b Discrete crack lengths (at experimental stopping instances) captured from Fig.9a

rates in the context of transient overloading. The slight under prediction in rate, compared to experimental values is attributed to the lack of continuous experimental data, which led to the use of an averaging technique for rate estimation over large numbers of cycles. Figure 9A shows the continuous crack length estimated for different samples and Fig. 9B shows the crack lengths at discrete instances (where experimental data were collected) captured from Fig.9A. Comparing Figs. 9B and 5, it is found that the prediction accuracy improves over direct crack length based prediction as shown in Fig. 7B.

C. Gaussian Process On-line Prediction

For the on-line Gaussian Process prediction the input vector \mathbf{x}_i in the Eq. (4) is fed with sensor signal features found using either Principal Component Analysis or Kernel Principal Component Analysis. At each observation instant, N (ref. Eq. 1-5), the piezoelectric actuator as shown in Fig. 6 is actuated with a narrow band burst signal. The burst signal as shown in Fig. 10 has a central frequency of 135 KHz and a sampling frequency of 2Ms/sec. For each actuation, 150 sensor observations are obtained for probabilistic feature extraction. Out of the 150 sensor observations only 100 are used for the feature extraction. At any typical fatigue instances the representative sensor signals used for feature extraction are depicted in Fig. 11. These 100 observations are selected based on a Fast Fourier Transform filter that

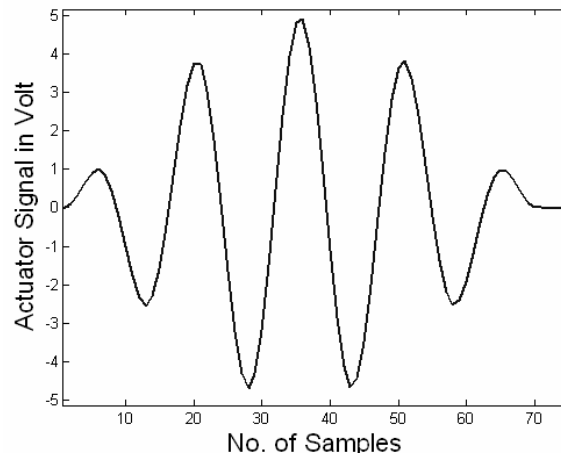


Fig. 10 Burst signal applied through PZT actuator

allows selecting a particular sensor signal with a central frequency in a range of 135 ± 30 KHz. The selection of 30 KHz upper and lower limit is based on the assumption that the maximum frequency variation of the observed signal will not cross these limits over the fatigue loading envelope. This ensures that signals containing only low frequency

noise due to the hydraulic pump of the fatigue frame or high frequency noise due to other environmental factors are not selected in the feature extraction process. Once the first 100 sensor signals of 1000 samples each, are selected, those signals are used as input in the feature extraction algorithm. With this information the value of 'M' and 'd' in expression

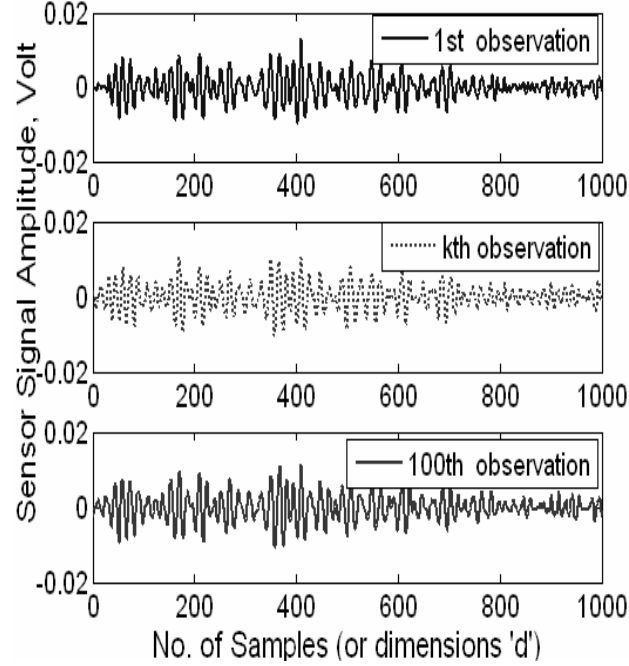
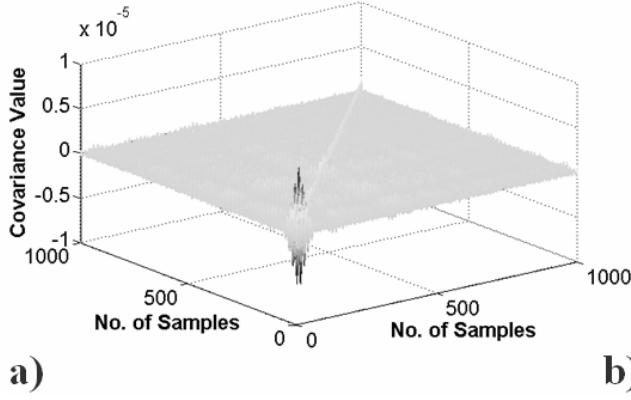


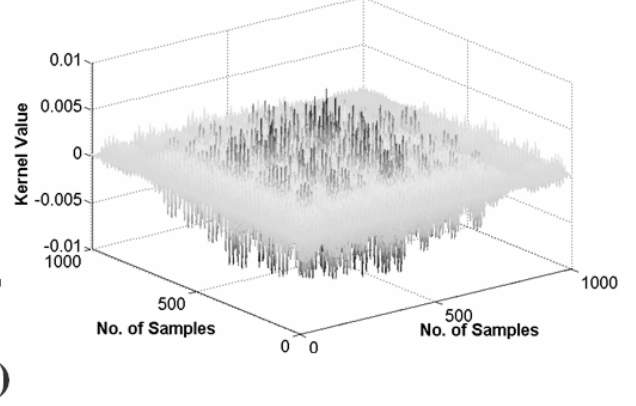
Fig. 11 Representative Sensor Signal for Feature Extraction

$\{\mathbf{y}_p \in R^M \mid p = 1, 2, \dots, d\}$ becomes $M=100$ and $d=1000$. The reason for selecting 100 similar observations for feature extraction is to statistically select the best features from the original signal, which may have buried environmental noise. Using the above mentioned signals, the covariance matrix (Eq. 6) for PCA and the kernel matrix (Eq. 8) for KPCA are evaluated. The covariance matrix for PCA and the Kernel matrix for KPCA at a typical observation instance are



a)

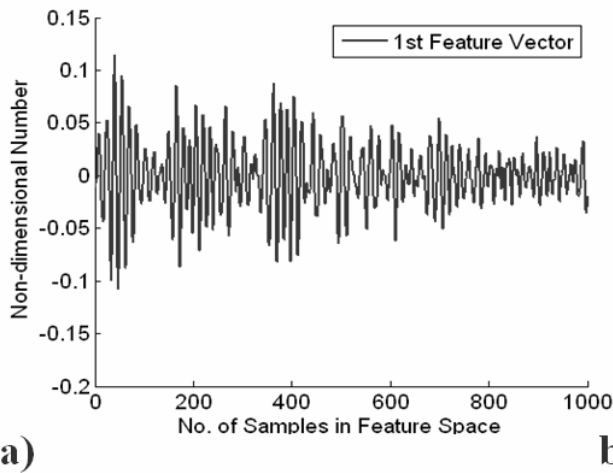
Fig. 12a Covariance at a typical fatigue instance for Principal Component Analysis



b)

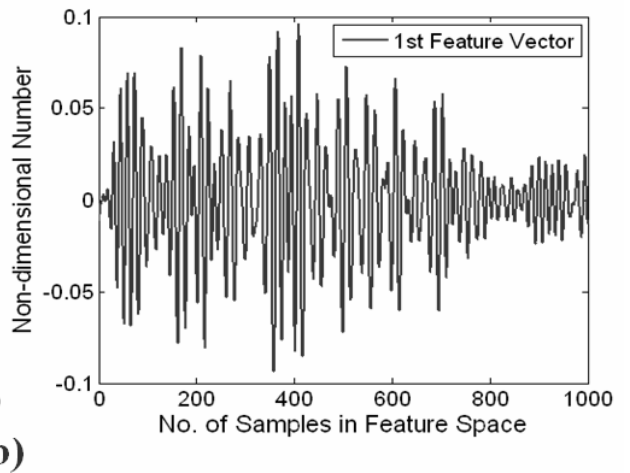
Fig. 12b Kernel at a typical fatigue instance for Kernel Principal Component Analysis

shown in Figs. 12a and 12b, respectively. The covariance matrix is used to solve the eigenvalue problem described in Eq.(7) for PCA based feature extraction, and the kernel matrix is used to solve the eigenvalue problem described in Eq.(9) for KPCA based feature extraction. From the eigenvalue analysis the first eigenvector is selected as the feature vector. It must be noted that the feature extraction is done at each discrete instance, where the fatigue frame was stopped to collect data. This leads to 'N' (Eq. 1-5) number of feature vectors, each of length $d=1000$. The first feature vectors at typical fatigue instance found from PCA and KPCA are respectively shown in Fig. 13a and 13b.



a)

Fig. 13a First feature vector from PCA



b)

Fig. 13b First feature vector from KPCA

Once the feature vectors are obtained for different instances, the Gaussian process input and output space are formed. The input training space of size $d \times N$ is formed from the 'N' feature vectors. The corresponding training output space consists of 'N' observed crack length, which are used in the off-line prediction. Once the Gaussian

process training input and output spaces are formed the prediction of an unseen output state, here the crack length or crack growth rate, is made using Eq. 2-5. Unlike the log scaling of both input and output spaces used for the off-line prediction, for the on-line prediction the input space is not scaled, but the output space is scaled with zero mean, unit variance scaling. This type of scaling is performed to ensure that both the input and the output spaces have similar variances, though not necessarily the same. It is noted that the Gaussian process works well when the distribution of underlying variables have similar mean and variances. The results for direct crack length predicted using PCA based feature extraction technique is shown in Fig. 14, and results with the KPCA based feature extraction technique is shown in Fig.15. The figures indicate that the match between experiment and prediction is not as good for all the fatigue loading envelopes as seen for the off-line prediction, but there is the same qualitative trend between experiment and prediction, particularly during the transient fatigue loading phase. This is because during the transient over load regime larger numbers of data points are available (ref. Fig.5) compared to the lower load regime. During the lower load regime the crack growth is assumed stable and hence fewer data points are collected over this

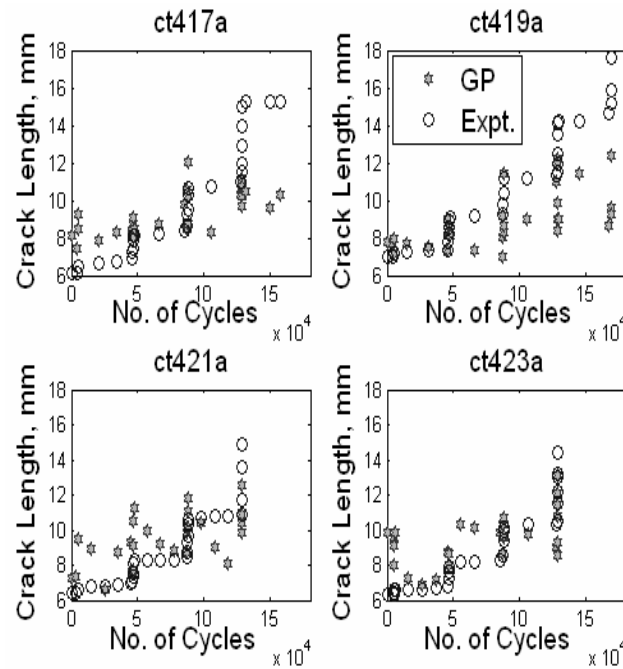


Fig. 14 Direct crack length prediction using PCA features

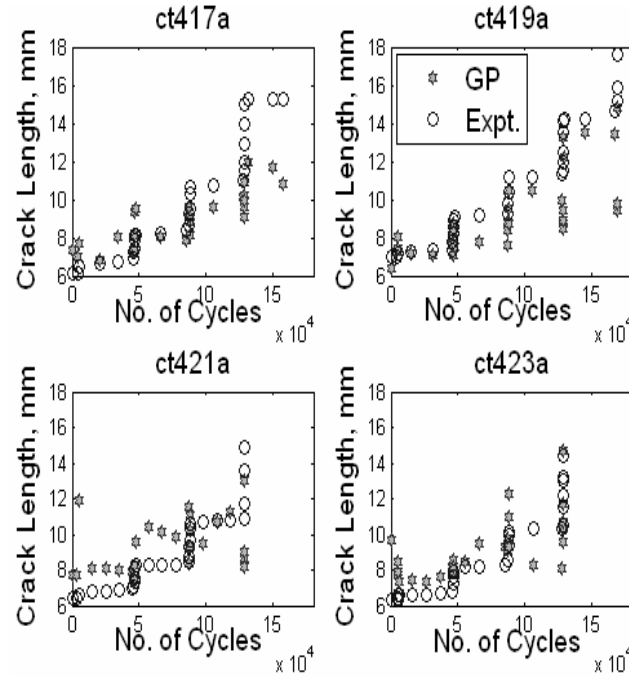


Fig. 15 Direct crack length prediction using KPCA features

regime. In addition, the crack growth rate during lower load regime is approximately one and half order of magnitude less compared to the average crack growth rate during the transient high load regime. For example for the ct423a sample, the average crack growth rate during the lower load regime is approximately 1.041×10^{-5} mm/cycles, whereas the approximate average rate during the third high load regime (87e3 to 88e3 cycles) is 1.4×10^{-4} mm/cycles. This possibly leads to a Gaussian Process scaling mismatch and subsequent erroneous prediction in the lower load regime. The scaling issues will be addressed during our future work. Crack growth rates are also predicted using the Gaussian Process based on-line predictive model. The crack growth rates are predicted using both PCA and KPCA based feature extraction techniques, and are shown in Fig. 16 and 17, respectively. The figures indicate that unlike

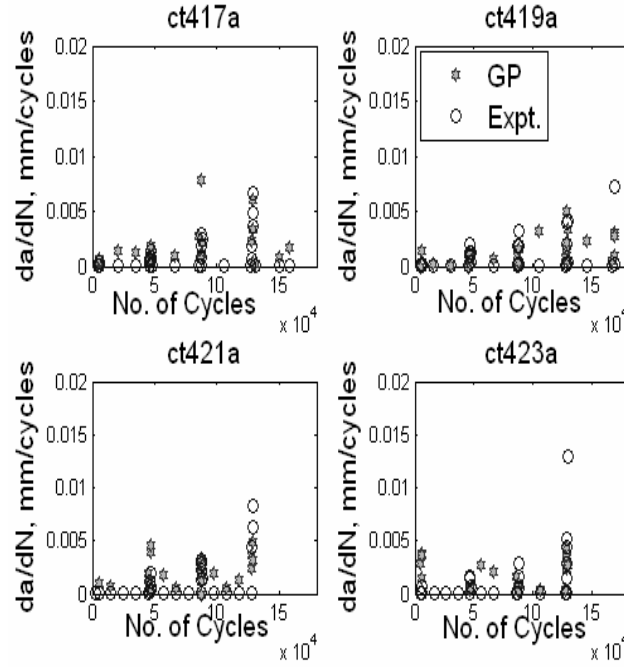


Fig. 16 Crack growth rate prediction using PCA features

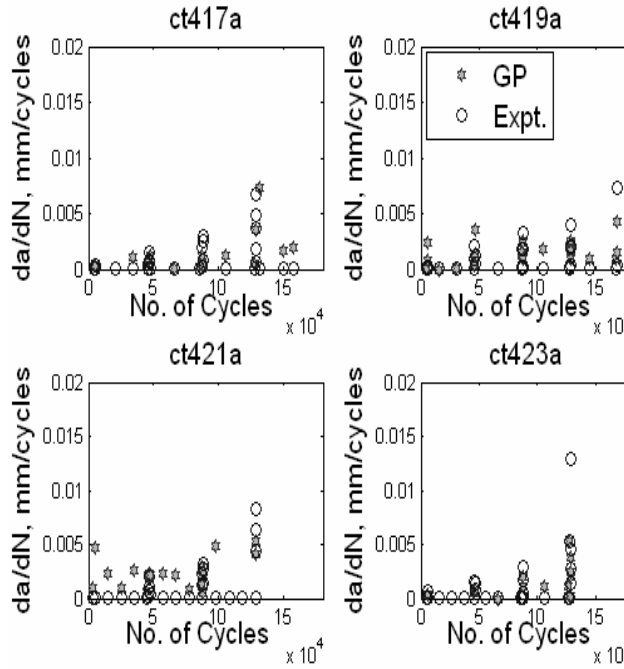


Fig. 17 Crack growth rate prediction using KPCA features

the case of direct crack growth prediction, in the crack growth rate prediction there is better correlation between experimental and predicted rates. Also it is found that both the feature extraction algorithms produce similar results on crack growth rate prediction, except in the case of the ct423a specimen. For this specimen, the GP prediction of

the rate with KPCA bond features correlates better with experiment compared to PCA based GP prediction. The KPCA based GP prediction could possibly be improved further by using a non stationary kernel (e.g. Eq. 4) as opposed to the stationary kernel (Eq.9) used for the present feature extraction problem, which will be our future work. Once the crack growth rates are predicted using GP, the continuous crack length can be estimated via cycle by cycle integration of the predicted rates. In the absence of rate information at any particular cycle, a strategy similar to that for the off-line prediction is employed to estimate the corresponding crack length. However, it is noted that for the online prediction case, while estimating the crack length in the lower load regime the integration algorithm is modified to select the minimum between the GP predicted rate and a rate of value 1.041×10^{-5} mm/cycles. This value is found from experimental observations in the lower load regime of CT423a samples, but is of similar value for other samples. The purpose of using this value in the integration process is to avoid using a spurious rate as predicted from the GP particularly in a lower load regime. The continuous crack lengths as integrated from the predicted rate are shown Fig. 18 and 19, respectively, for PCA and KPCA based predictions. Figures 14, 15, 18 and 19 show that for both the PCA and the KPCA based feature extraction techniques, the rate-based prediction of crack length growth has better correlation with experiments compared to the direct GP prediction of crack growth.

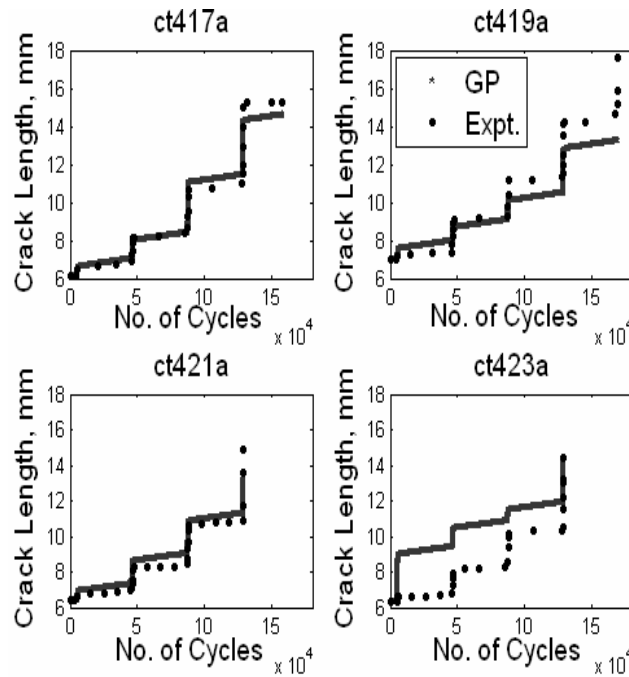


Fig. 18 Estimated crack length using PCA features

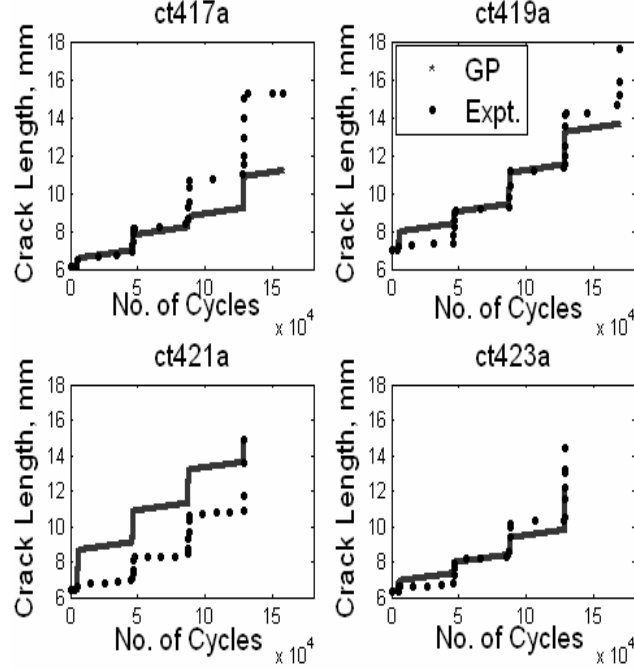


Fig. 19 Estimated crack length using KPCA features

IV. Concluding Remarks

Off-line and On-line data driven (probabilistic) models are proposed for the future hybrid prognosis framework. The proposed probabilistic multivariate Gaussian Process approach within a Bayesian framework has been used to investigate the fatigue crack behavior of Al 2024 compact-tension (CT) specimens under variable loading. The input space of the model is trained with parameters such as number of fatigue cycles, minimum load, maximum load, and load ratio for the off-line prediction. Whereas, the input space is trained using features obtained from piezoelectric sensor signals for the online prediction. In both off-line and on-line cases, the output space is trained with known associated crack lengths. Using the trained Gaussian Process model predictions are made for the unknown output space (crack length or crack growth rate) and the results are validated with experiments. Some important observations from this study are as follows:

1. The numerical results indicate that the multivariate off-line prediction model outperforms the single variate prediction model.
2. The rate based Gaussian Process crack growth prediction better captures the physics of the dynamic system, under variable loading condition.

3. The on-line architecture developed is used to evaluate the performance of PCA and based feature extraction algorithms. It is found that in some cases the PCA based prediction algorithm gives better predictions, whereas in others the KPCA based prediction performs better. The consistency in kernel based algorithm for better prediction will be investigated in future work.
4. The on-line prediction algorithms are used to validate a realistic situation, where the component under investigation is an integral part of a larger structural assembly (in the present case the fatigue frame).
5. In the present framework, using the Bayesian based probabilistic approach the uncertainty due to loading, and microstructural parameters is explicitly modeled in the prediction algorithm. In the future the off-line Gaussian Process model will be combined with a physics-based model to further improve the prediction accuracy and horizon.

Acknowledgments

This research was supported by the MURI Program, Air Force Office of Scientific Research, grant number: FA9550-06-1-0309; Technical Monitor, Dr. Victor Giurgiutiu.

References

- ¹Hess, A., Calvello, G., Frith, P., Engel, S.J., and Hoitsma, D., "Challenges, Issues, and Lessons Learned Chasing the "Big P": Real Predictive Prognostics Part 2," *Proceedings of IEEE Aerospace Conference*, AERO.2006.1656124, Vol. 4-11, March 2006, pp. 1 – 19.
- ²Hess, A., and Frith, P., "The Joint Strike Fighter (JSF) PHM Concept: Potential Impact on Aging Aircraft Problems," *Proceedings of IEEE Aerospace Conference*, AERO.2002.1036144, Vol. 6, 2002, pp. 6-3021 - 6-3026.
- ³Newman, J.C., Jr., "Prediction of fatigue crack growth under variable-amplitude and spectrum loading using a closure model," *ASTM STP*, Vol. 761, 1982, pp. 255-277 .
- ⁴Newman, J.C. Jr., "A crack-opening stress equation for fatigue crack growth," *International Journal of Fracture*, Vol. 24, 1984, R131-R135 .
- ⁵Newman, J.C. Jr., "FASTRAN-II - A Fatigue Crack Growth Structural Analysis Program," Langley Research Center, NASA TM 104159, 1992.
- ⁶Harter, J.A., "AFGROW Users' Guide and Technical Manual," Air force Research Laboratory, AFRL-VA-WP-1999-3016, 1999.
- ⁷Miner, M. A., "Cumulative Damage in Fatigue," *Journal of Applied Mechanics*, Sept. 1945, pp. A-159 - A-164.

- ⁸ Samborsky, D.D, Wilson, T.J., and Mandell, J.F., “Comparison of Tensile Fatigue Resistance and Constant Life Diagrams for Several Potential Wind Turbine Blade Laminates,” *Proceedings of Wind Energy Symposium*, Reno, Nevada, Jan. 2007.
- ⁹ Zapatero, J., and Domnguez, J., “A statistical approach to fatigue life predictions under random loading,” *International Journal of Fatigue*, Vol. 12, No. 2, 1990, pp. 107-114.
- ¹⁰ Yongming, L., and Sankaran M., “Stochastic fatigue damage modeling under variable amplitude loading,” *International Journal of Fatigue*, Vol. 29, No. 6, June 2007, pp. 1149-1161.
- ¹¹ Elber W., “Fatigue crack closure under cyclic tension,” *Engineering Fracture Mechanics*, Vol. 2, 1970, pp.37-45.
- ¹² Ray, A., and Patankar, R.P., “Fatigue Crack Growth Under Variable Amplitude Loading-Part-I: Model Formulation in State-Space Setting,” *Applied Mathematical Modeling Journal*, Vol. 25, No. 11, Nov. 2001, pp. 979-994.
- ¹³ Ray, A., and Patankar, R.P., “Fatigue Crack Growth Under Variable Amplitude Loading-Part-II: Code Development and Model Validation,” *Applied Mathematical Modeling Journal*, Vol. 25, No. 11, Nov. 2001, pp. 995-1013.
- ¹⁴ Ioannis, A., and Ilias M., “Neural network-based diagnostic and prognostic estimations in breast cancer microscopic instances,” *Medical and Biological Engineering and Computing*, Vol. 44, No. 9, Sept. 2006, pp. 773-784.
- ¹⁵ Vachtsevanos, G., and Wang, P., “Fault prognosis using dynamic wavelet neural networks,” *Proceedings of IEEE Systems Readiness Technology Conference*, AUTEST.2001.949467, 2001, pp. 857 – 870.
- ¹⁶ MacKay, D.J.C., “Bayesian Interpolation”, *Neural Computation*, Vol. 4 , No. 3, 1992, pp. 415-447.
17. MacKay, D.J.C., *Introduction to Gaussian processes*, Edited by C. M. Bishop, *Neural Networks and Machine Learning*, NATO ASI Series, Springer, Berlin, 1998, Vol. 168, pp. 133-165.
18. Rasmussen, C., and Williams C., *Gaussian Processes for Machine Learning*, The MIT Press, Cambridge, MA, 2006.
19. Smith, L., “A tutorial on Principal Component Analysis,” [online database], URL: http://www.cs.otago.ac.nz/cosc453/student_tutorials/principal_components.pdf, [cited 2002].
20. Rao, C.R. “The Use and Interpretation of Principal Component Analysis in Applied Research,” *Sankhya*, Vol. A 26, 1964, pp. 329-358.
- 21 Scholkopf, B., Smola, A., and Muller, K., “Nonlinear Component Analysis as a Kernel Eigenvalue Problem”, [online database], Technical Report No. 44, Max-Planck-Institute, Tubingen, Germany, URL: http://www.face-rec.org/algorithms/Kernel/kernelPCA_scholkopf.pdf, [cited December 1996].
22. Mohanty, S., Das, S., Chattopadhyay, A., and Peralta, P., “Gaussian Process Time Series Model for Life Prognosis of Metallic Structure”, Accepted for publication in *Journal of Intelligent Material Systems and Structures*.
23. Christopher K. I. Williams. “Computing with infinite networks,” Edited by Michael C. Mozer, Michael I. Jordan, and Thomas Petsche, *Advances in Neural Information Processing Systems*, MIT Press, Cambridge, MA, 1997, Vol. 9.